water

MDPI

Article

Sorption of 2,4-Dichlorophenoxyacetic Acid from Agricultural Leachate Using Termite Mound Soil: Optimization Using Response Surface Methodology

Yalemtsehay Debebe [1,2], Esayas Alemayehu [3,4,*], Zemene Worku [1], Wookeun Bae [5] and Bernd Lennartz [6,*]

[1] Department of Environmental Engineering, Addis Ababa Science and Technology University, Addis Ababa P.O. Box 16417, Ethiopia
[2] Department of Integrated Watershed Management, Jimma Agricultural Research Center, Jimma P.O. Box 192, Ethiopia
[3] Faculty of Civil and Environmental Engineering, Jimma University, Jimma P.O. Box 378, Ethiopia
[4] Africa Center of Excellence for Water Management, Addis Ababa University, Addis Ababa P.O. Box 1176, Ethiopia
[5] Department of Civil and Environmental Engineering, Hanyang University, Ansan 425-791, Kyunggi-do, Republic of Korea
[6] Faculty of Agricultural and Environmental Sciences, University of Rostock, Justus-Von-Liebig-Weg 6, 18059 Rostock, Germany
* Correspondence: esayas16@yahoo.com (E.A.); bernd.lennartz@uni-rostock.de (B.L.)

Abstract: The extensive use of 2,4-dichlorophenoxyacetic acid (2,4-D) pesticide leads to the contamination of surfaces and groundwater. In this respect, it is critical to develop an inexpensive and environmentally friendly adsorbent for 2,4-D-laden agricultural leachate. In the current study, termite mound soil (TMS) from Ethiopia was used as an adsorbent in a batch mode aimed at the removal of 2,4-D from an aqueous solution. The TMS was characterized using Brunauer–Emmett–Teller (BET), Fourier-transform infrared (FTIR), scanning electron microscopy (SEM), atomic absorption spectrometry (AAS), and X-ray diffraction (XRD) techniques. The effects of various operating parameters such as pH, contact time, adsorbent dose, and initial concentration were investigated. In addition, the optimization process and interaction effect were studied using response surface methodology (RSM). A high 2,4-D removal percentage (89.6%) was achieved for a 2,4-D initial concentration of 50.25 mg/L at pH 2, an adsorbent dose of 15.25 g/L, and a contact time of 180.5 min. The 2,4-D adsorption isotherms could be adequately described by the Langmuir model (R^2 = 0.9687), while the kinetics of the 2,4-D adsorption on the TMS best fit the pseudo-second-order model. Overall the study showed that TMS is an effective adsorbent for the removal of 2,4-D from agricultural leachate.

Keywords: agricultural leachate; 2,4-D; termite mound soil; adsorptive removal

check for updates

Citation: Debebe, Y.; Alemayehu, E.; Worku, Z.; Bae, W.; Lennartz, B. Sorption of 2,4-Dichlorophenoxyacetic Acid from Agricultural Leachate Using Termite Mound Soil: Optimization Using Response Surface Methodology. *Water* **2023**, *15*, 327. https://doi.org/10.3390/w15020327

Academic Editors: Anna Wołowicz and Monika Wawrzkiewicz

Received: 19 December 2022
Revised: 8 January 2023
Accepted: 9 January 2023
Published: 12 January 2023

1. Introduction

Biological creatures, such as weeds, insects, and rodents, can be killed by a wide range of compounds known as pesticides [1]. Chemical pesticides have been used in agriculture for decades to lower crop loss and fulfill the rising global food demand. According to [2], almost one-third of farm products are produced using chemical pesticides. Pesticides include a variety of substances, such as insecticides, fungicides, herbicides, rodenticides, molluscicides, nematicides, plant growth regulators, and others. Of these, 2,4-D is the most widely used herbicide due to its low cost, selectivity, efficiency, and wide range of weed control [2,3]. However, because of its high water solubility, acidic characteristics, and mobility, it has become a serious problem for soil and groundwater contamination [4]. It recommends a maximum of 10 mg/L in leachates from soils and wastes since it has a serious, detrimental effect on the environment [5]. Surfaces and groundwater have

become contaminated due to the widespread usage of 2,4-D [6], which denotes a serious environmental issue and health risk [2,7].

Therefore, it is crucial and significant to create a technology that removes 2,4-D herbicides effectively. Several methods include electrochemical oxidation, catalytic reactions (oxidation and ozonation), Fenton degradation, photocatalytic degradation, and bioremediation [6,8]. Electrochemical treatment results in the complete mineralization of the 2,4-D pollutant in a short period of time. However, these technologies are expensive, and due to the non-selective process, toxic byproducts can be created [9]. Likewise, catalytic reactions (oxidation and ozonation) can totally destroy 2,4-D, but they demand a large amount of energy and have a relatively short useful life for the degrading agent (hydrogen peroxide or ozone). This makes it more difficult to apply the processes on a wide scale [9]. Due to the metallic oxidation states, such as Fe (III) and Fe (III) $(OH)^{2+}$, Fenton is able to degrade the 2,4-D anion in as little as 40 min. However, this requires pH adjustment before using the catalyst in situ, and maintaining the operational conditions, such as pH and catalyst synthesis, is expensive [10].

The photocatalytic degradation process and operating conditions are simple, making it easy to use. In comparison to most other processes, the photocatalytic reaction takes less time. The removal percentage is also high. However, the practical use of this technique is hampered by the necessity of a very potent UV light source and a catalyst with high activity [9]. On the other hand, bioremediation, which uses naturally occurring biological activity to decontaminate 2,4-D, is secure, relatively low-cost, and generally well-accepted by the general public. However, the time scales involved are relatively long and, during the biotransformation process, intermediates are formed, which can sometimes be more toxic than the parent [11]. Due to the drawbacks of the above-discussed technologies, adsorption using low-cost, locally available materials, with easy operation and design, has been considered highly efficient and well-accepted for the 2,4-D removal process by researchers in recent years [7,8,12]. The adsorbents used to remove pesticides include clays, polymeric materials, synthetic and commercial activated carbons, as well as agricultural and industrial waste [13]. Some of the adsorbents mentioned above (activated carbons) are costly to manufacture and regenerate, while others are difficult to obtain in bulk, which has occasionally limited their utilization [14].

Hence, studies have been going on to explore simple, low-cost, efficient, and socially acceptable methods for the effective removal of pesticides from agricultural leachate. In this context, TMS, which is abundant in Ethiopia, could be a good addition to enhance the remediation of 2,4-D from agricultural leachate. TMS is found frequently and abundantly in the farmland of Ethiopia. There are 12 mounds, on average, per hectare, and the average mound soil mass is calculated to be 58.9 tons [15]. Minerals and soil nutrients (phosphorus, sulfur, and organic matter) have been shown to be more abundant in termite mound soil than in nearby soil [16], and TMS are also hotspots for bacterial concentration. Native microorganisms utilize the phosphorus in the TMS for cell expansion, which increases their activity to break down pesticides. Moreover, the surface characteristics and mineralogical composition of TMS could position it as an excellent adsorbent [17].

However, the adsorption of 2,4-D herbicide from agricultural leachate by TMS has not been reported yet. Particularly, the process parameters for 2,4-D removal by TMS have not been optimized. Response surface methodology (RSM) has been used to optimize procedures and product design by combining statistical design and numerical optimization techniques [18]. The main advantages of this method are reducing the number of experimental trials and calculating the complex interaction between the independent variables, analysis, and optimization, as well as the improvement of the existing design [19]. To the best of our knowledge, no information exists with respect to the adsorption capacity of TMS for the removal of 2,4-D from agricultural leachate using RSM. Therefore, the current study's primary objective was to explore the effectiveness of TMS in removing 2,4-D from agricultural leachate by optimizing process factors such as pH, adsorbent (TMS) dose, initial 2,4-D concentration, and contact time using response surface methodology.

Moreover, the adsorption isotherm and adsorption kinetics of 2,4-D adsorption on the TMS were investigated.

2. Materials and Methods

2.1. Adsorbent Preparation

Six different termite mound soil samples were collected from Meki town, East Shewa zone, Oromia region, Ethiopia. The samplings were done from the top, middle, and bottom parts of the parent soil, and then mixed in equal proportions. Dust and other tiny particles from the TMS sample were thoroughly and repeatedly washed away prior to the sorption experiment. The moist sample was then dried for 1440 min at a temperature of 105 °C [20]. Finally, the ground and sieved (0.075 mm) sample was kept in a desiccator until the experiment began to prevent moisture absorption.

2.2. Adsorbent Characterization

The oxide and elemental (Ni, Pb, and Cd) compositions of the TMS were analyzed using an atomic absorption spectrometer (AAS) and flame atomic absorption spectroscopy (FAAS), respectively. The total carbon, total nitrogen, and total sulfur contents were analyzed in a soil sample using ES ISO 14,235 (2015), ES ISO 11,261 (2015) (Kjeldahl), and the turbidimetric procedure ISO 11,466 (1995), respectively. Using a pH meter with a combination of gel-filled glass electrodes, the pH of the adsorbent in water (soil-to-solution ratio: 1:2.5) was determined [20]. Techniques that entailed adding salt were used to find the point of zero charge [21]. In this method, the sample (0.2 g) and 0.1 $MNaNO_3$ (40 mL) were mixed in 10 vessels. The pH was adjusted to an initial pH of 3, 4, 5, 6, 7, 8, 9, 10, 11, and 12 using 0.1 M HNO_3 and 0.1 M NaOH. Then, the beaker was shaken for 24 h on an orbital shaker at 150 rpm. Each resulting pH was measured after settling, and the gap between the initial and final pH values (ΔpH) was displayed, taking the pzc value as the point where ΔpH = 0 [21].

Using a surface area analyzer (SA-9600 Horiba), the surface area of the TMS was calculated based on the nitrogen gas isotherms of adsorption and desorption at a 700 mm atmospheric pressure [22]. The surface morphology of the adsorbent was investigated by applying scanning electron microscopy (SEM). The SEM INSPECTIF 50 machine was used for the analysis, with a beam size of 7 and 10, and 3000 and 9000× magnifications [22]. The functional group on the surface of the TMS was examined using the FTIR spectrophotometer, which was scanned in the 400–4000 cm^{-1} range [23]. The TMS was investigated utilizing an X-ray diffractometer model (XRD-7000, Shimadzu Corporation, Japan) with a range of 10–90 (2θ) for characterizing the crystal structure and mineral content.

2.3. Sorption Experiment

The batch sorption experiment [24] was carried out using a synthetic aqueous solution that contained 2,4-D. In order to create the 2,4-D-containing synthetic solution, 1.0 g of 2,4-D (powder, technical grade) was dissolved in 1 L of distilled water to achieve a 1000 mg/L concentration. This aqueous solution has then undergone the proper dilutions to achieve the required concentrations. A ceramic magnetic stirrer (JIJE LAB GLASS) was used to stir a solution containing a known amount of 2,4-D and the necessary amount of TMS at 250 revolutions per minute. The remaining 2,4-D concentration was then calculated using an Agilent Cary 60 UV/Visible spectrophotometer at 282 nm after the liquids were spun at 3500 rpm for 15 min [3]. The difference between the concentrations of the beginning and final solutions was used to calculate the quantity of 2,4-D adsorbed on the TMS.

2.3.1. Effect of Contact Time

A quantity of 15.25 g/L of the TMS sample was weighed into a centrifuge tube. The addition of the solution containing 50.25 mg/L 2,4-D was followed by a measurement of the effect of the contact time by adjusting the agitation duration from 0 to 360 min while

maintaining the other parameters constant. The adsorption capacity (q_t) and removal percentages (A%) were computed using Equations (1) and (2), respectively [25].

$$q_t = \left(\frac{C_0 - C_t}{M}\right) \times V \tag{1}$$

$$A\% = \left(\frac{C_0 - C_t}{C_0}\right) \times 100 \tag{2}$$

where C_t (mg/L) is the concentration of 2,4-D in the aqueous phase at any time, t; q_t (mg/g) is the quantity of 2,4-D adsorbed at any time, t (min); A (%) is the percentage of 2,4-D removed; C_0 (mg/L) is the initial 2,4-D concentration; V (L) is the volume of the aqueous solution; and M (g) is the mass of adsorbents used in the experiment.

2.3.2. Effect of pH

By allowing 15.25 g/L TMS to adsorb 50.25 mg/L 2,4-D in the aqueous solution while maintaining the other parameters constant, the influence of the solution pH was examined.

2.3.3. Effect of TMS Dose

By changing the amount of TMS from 0.5 g/L to 30 g/L, while maintaining the same values for the other parameters, the impact of the adsorbent dosage on the removal of 2,4-D was investigated.

2.3.4. Effect of 2,4-D Concentration

By changing the concentration of 2,4-D from 0.5 mg/L to 100 mg/L, while holding the other variables constant, the initial concentration effect was assessed.

2.4. Adsorption Kinetics

The adsorption kinetics were analyzed using the pseudo-first-order, pseudo-second-order, and intraparticle diffusion models, which are represented by Equations (3–5), respectively [26].

$$\ln(q_e - q_t) = \ln q_e - K_t \tag{3}$$

$$\frac{t}{q_t} = \frac{1}{K_2 q_e 2} + \frac{t}{q_e} \tag{4}$$

$$q_t = k_p t^{1/2} + C \tag{5}$$

where q_e is the equilibrium mass of adsorbed 2,4-D (mg/g); q_t is the adsorption quantity at time t (mg/g); K (min^{-1}) is the first-order rate constant; K_2 (g/(mg.min)) is the second-order rate constant; K_p (mg/(g.$min^{0.5}$)) is the intraparticle rate diffusion constant; and C (mg/g) is the intraparticle diffusion model's intercept.

2.5. Adsorption Isotherm

The Langmuir model Equations (6) and (7), and the Freundlich model Equations (8) and (9), respectively, were used to fit the adsorption data [27].

$$q_e = \frac{q_{maxbC_e}}{1 + bC_e} \tag{6}$$

The constants in the Langmuir isotherms were obtained by plotting $1/q_e$ vs. $1/C_e$ and using the equation above, which is now written as:

$$\frac{C_e}{q_e} = \frac{1}{q_{max} b} + \frac{C_e}{q_{max}} \tag{7}$$

The Langmuir constant (b) and the maximum adsorption capacity (q_{max}) of the adsorbent (mg/g) were calculated using the slope and intercept of the line that was obtained from the plot of $1/q_e$ versus $1/C_e$.

Where q_e is the quantity of 2,4-D sorbed at equilibrium per unit mass of adsorbents (mg/g), C_e is the concentration of 2,4-D in the liquid phase (mg/L).

$$q_{e} = K_f Ce^{1/n} \tag{8}$$

The constants in the Freundlich isotherms were found by graphing log q_e vs.log C_e and using the preceding equation, which is now written as:

$$\log q_{e} = \log K_f + 1/n \log C_e \tag{9}$$

where 1/n is a dimensionless parameter known as the adsorption constant, and K_f is the Freundlich coefficient.

2.6. Response Surface Modeling and Experimental Design

The optimal conditions for the adsorption of 2,4-D by the TMS adsorbent were discovered using a central composite design (CCD) under RSM. Using four different variables as inputs, optimization experiments were conducted (pH, contact time, adsorbent dose, and initial concentration of 2,4-D). Design–Expert software version 13 (Stat-Ease Inc., Minneapolis, MN, USA) was used to construct the mathematical model. In a half-factorial CCD design which produced 21 tests, each factor was examined. Table 1 provides the components and levels.

Table 1. Factors and levels designed to remove 2,4-D in percentage.

Name (Factor)	Units	Low (−)	Middle (0)	High (+)	−α	+α
pH (A)		2	5.5	9	1.5	12.5
Contact time (B)	Minute	1	180.5	360	121.4	482.4
Adsorbent dose (C)	g/L	0.5	15.25	30	9.6	40.1
Initial 2,4-D concentration (D)	mg/L	0.5	50.25	100	33.4	133.9

Equation (10) [28] represents the quadratic equation model for estimating the optimal.

$$Y = \beta_0 + \sum_{i=1}^{k} \beta_i X_i + \sum_{i=1}^{k} \beta_{ii} X_i^2 + \sum_{i=1}^{k-1} \sum_{j=i+1}^{k} \beta_{ij} X_i X_j + \varepsilon \tag{10}$$

where Y is the response; β_0 is the constant coefficient; β_i, β_{ii}, and β_{ij} are the coefficients for the linear, quadratic, and interaction effects, respectively; X_i and X_j are the factors; and ε is the error.

3. Results and Discussion

3.1. Adsorbent Characterization

3.1.1. Chemical Composition

Table 2 lists the chemical components of the TMS. High levels of silicon, aluminum, and iron oxides make up 76.79 wt% of the mixture. The combined total carbon and total nitrogen value of the sample was 2.43 weight percent. The TMS also contains K_2O, CaO, and P_2O_5, which function as soil micronutrients [8].

Table 2. Chemical composition of TMS.

Content (%)	Value
SiO_2	60.36
Al_2O_3	10.25
Fe_2O_3	6.18
TiO_2	0.31
MgO	1.06
Na_2O	1.68
K_2O	2.74

Table 2. *Cont.*

Content (%)	Value
CaO	2.34
MnO	0.12
P_2O_5	0.33
SO_3	<0.01
LOI	8.38
Total C	2.3
Total S	ND
Total N	0.13
Pb	ND
Ni	ND
Cd	ND

ND: Indicates not detected.

3.1.2. Point of Zero Charge (pHpzc)

The pH point of zero charge (pHpzc) of adsorbents is the pH level at which the overall charge of the entire particle surface equals zero [22]. As seen in the following, Figure 1, the TMS adsorbent's pHpzc was 7.5. As a result, it is anticipated that cationic pollutants will adsorb at pH levels greater than 7.5, while anionic pollutants can absorb at pH levels lower than 7.5. At pH 2, the TMS surface becomes positive. As a result, the pHpzc value supports the experimental results of 2,4-D adsorption, making the adsorbent vulnerable to 2,4-D adsorption through electrostatic attraction.

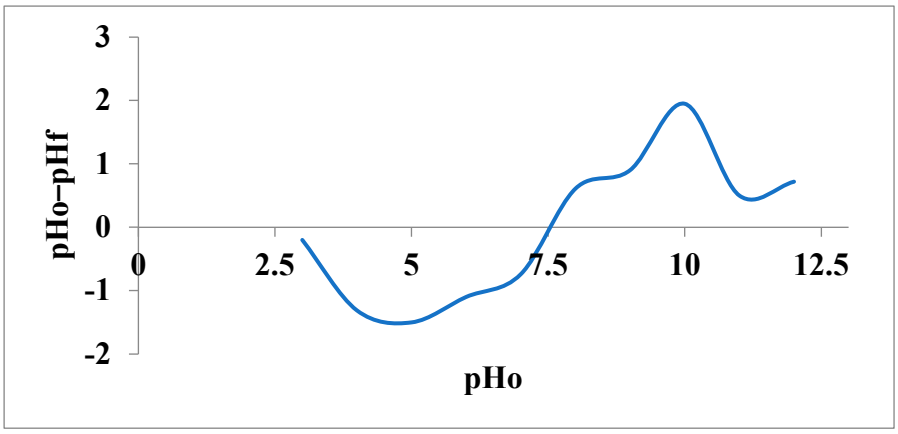

Figure 1. TMS adsorbent's point of zero charge (pHpzc).

3.1.3. Specific Surface Area

The BET surface area of the TMS with particle sizes less than 0.075 mm was 28.5 m^2/g; 28.4 m^2/g was the prior study report for TMS [25].

3.1.4. SEM Examination

Prior to and following the adsorption, the TMS underwent SEM examination (Figure 2). The adsorption of 2,4-D on the surface of the TMS was demonstrated by the smoothing-out and filling-in of the pores and surface caves of the soil, as illustrated in Figure 2.

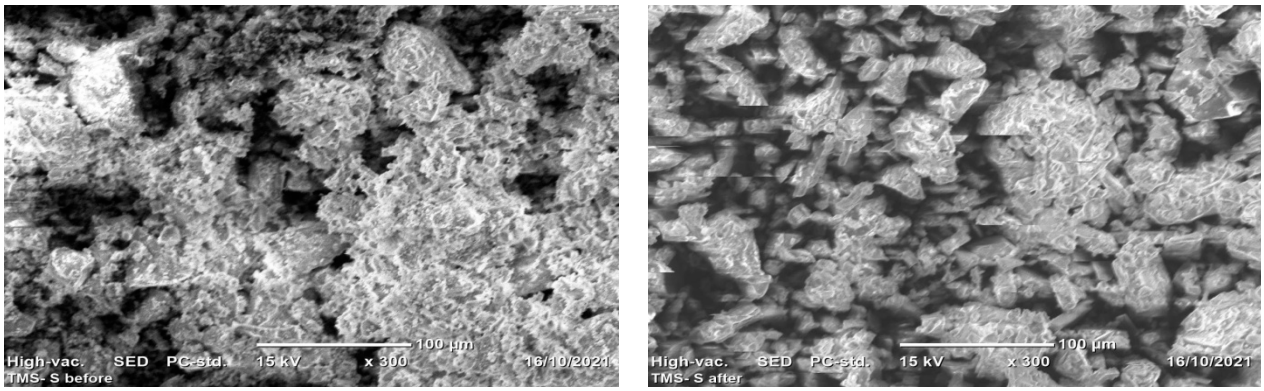

(**A**) (**B**)

Figure 2. TMS's surface morphology (**A**) prior to adsorption and (**B**) following adsorption.

3.1.5. FTIR Analysis

It is possible to identify the surface functional groups of adsorbents using Fourier-transform infrared spectroscopy [29]. Figure 3 displays the TMS FTIR spectra before and after adsorption. The bands at 1019 (Si-O stretching) show where substantial absorption occurs, in the range of 800–1200 cm^{-1} [30]. The Si-O-Si bond's tetrahedral bending vibration is attributed to the medium bands at 794 cm^{-1} and 463 cm^{-1}; this peak is typical of crystalline quartz [31]. The Si-O and Al-OH, two of the primary functional groups, were seen to vibrate in the 1000–500 cm^{-1} range. Figure 3 displays the 2,4-D spectra that have been adsorbed on the TMS (after adsorption), which clearly demonstrates the loss of peaks at 1452 cm^{-1} and the formation of new bands at 1645 cm^{-1}. Due to 2,4-D's transfer of electrons to the TMS surface, the peak has shifted. The existence of 2,4-D in the anionic form is confirmed by these new bands, which are caused by the 2,4-D anion's C=O vibration.

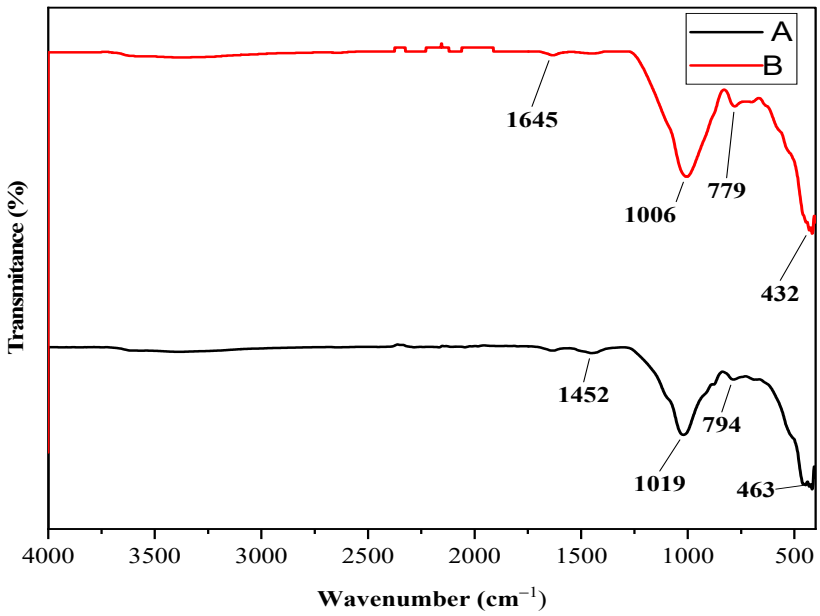

Figure 3. TMS Fourier-transform infrared (FTIR) (A) before adsorption and (B) after adsorption.

3.1.6. XRD Analysis

Figure 4 shows the TMS diffraction structure. The notable diffraction peak and corresponding angles are 12.45 (kaolinite), 20 (opal), 23.7 (hematite), 26.8 (quartz), 27.7 (feldspar), 29.7 (kaolinite), 35 (goethite), 47 (quartz), and 50 (calcite) found in the TMS [22,32]. From Figure 4, it can be concluded that the predominant element is quartz (SiO_2). This confirms the previous AAS result in Table 2.

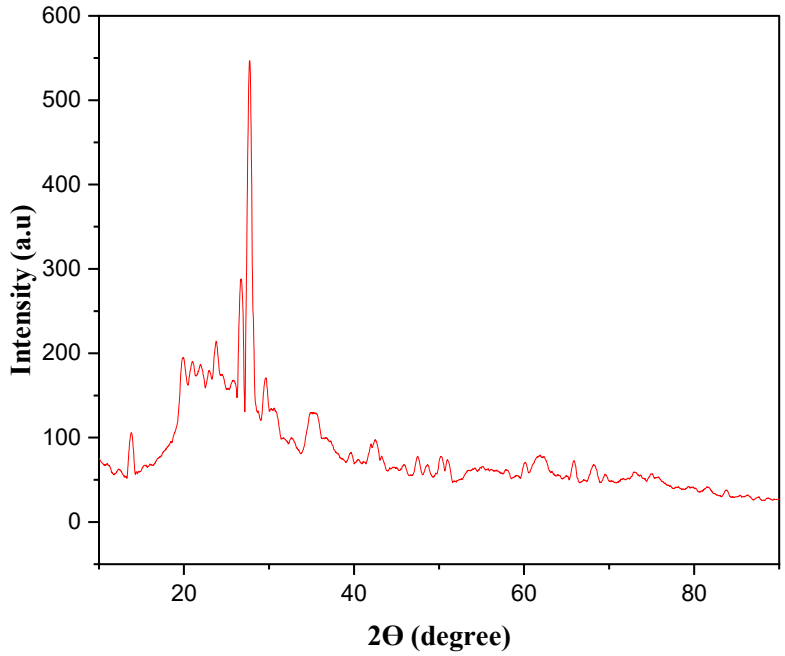

Figure 4. The TMS's XRD patterns.

3.2. 2,4-D Sorption

3.2.1. Effect of pH

The effect of pH on 2,4-D removal by the TMS is graphically represented in Figure 5. Figure 5 demonstrates that the highest 2,4-D adsorption capacity (q_e) and the percentage of 2,4-D removal (A%) by the TMS were observed at pH 2, which were 2.9 mg/g and 88%, respectively. The percentage of 2,4-D removal decreased significantly from 88 to 27%, as the solution pH increased from 2 to 9. The reduced adsorption at the basic pH is thought to be caused by the pesticide and adsorbent surfaces repelling one another [33]. The results are in line with those of a previous study [34], in which they discovered that the 2,4-D removal decreased when the pH increased from 2 to 7.5.

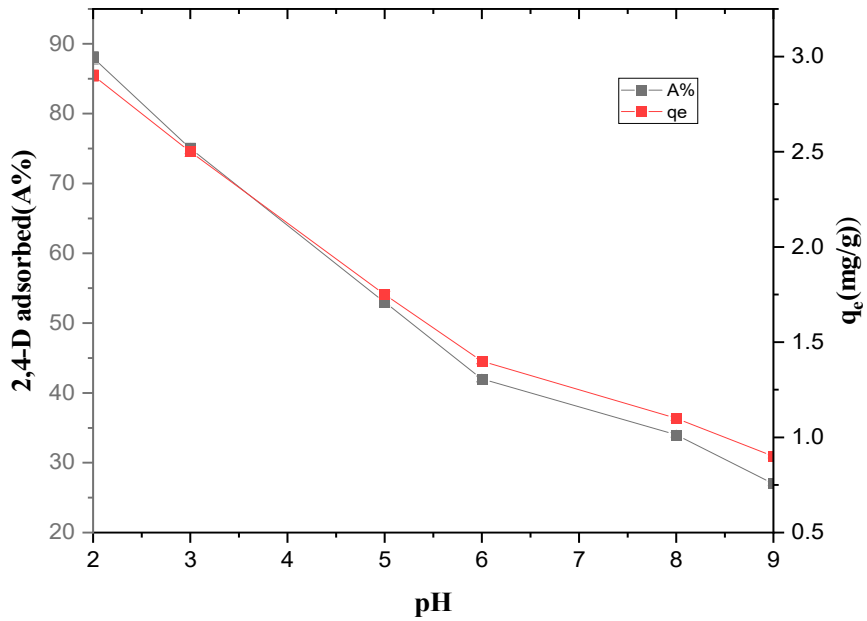

Figure 5. Effect of pH on 2,4-D percentage removal (A%) and adsorption capacity (q_e). The error bars show the standard deviation for three different sample runs.

3.2.2. Effect of TMS Dose

The influence of the adsorbent dose on the removal of 2,4-D was examined by increasing the amount of TMS from 0.5 g/L to 30 g/L while maintaining the concentration of 2,4-D at 50.25 mg/L. The percentage of 2,4-D removal and the adsorption capacity at different TMS dosages are shown in Figure 6. According to the findings, the adsorption capacity decreased from 44.2 to 1.01 mg/g with the increase in adsorbent dose from 0.5 to 30 g/L. The 2,4-D molecule had not completely covered the active sites of the TMS, and this was the main reason for the decrease in the adsorptive capacity value [12]. However, the percentage of 2,4-D removal increased rapidly from 44 to 80% as the adsorbent dose increased from 0.5 to 15.25 g/L, and, after 15.25 g/L, the percentage of removal decreased. As a result, 15.25 g/L was the TMS dose in this trial that gave the maximum 2,4-D removal percentage. Similar findings have been reported in previous studies [35,36].

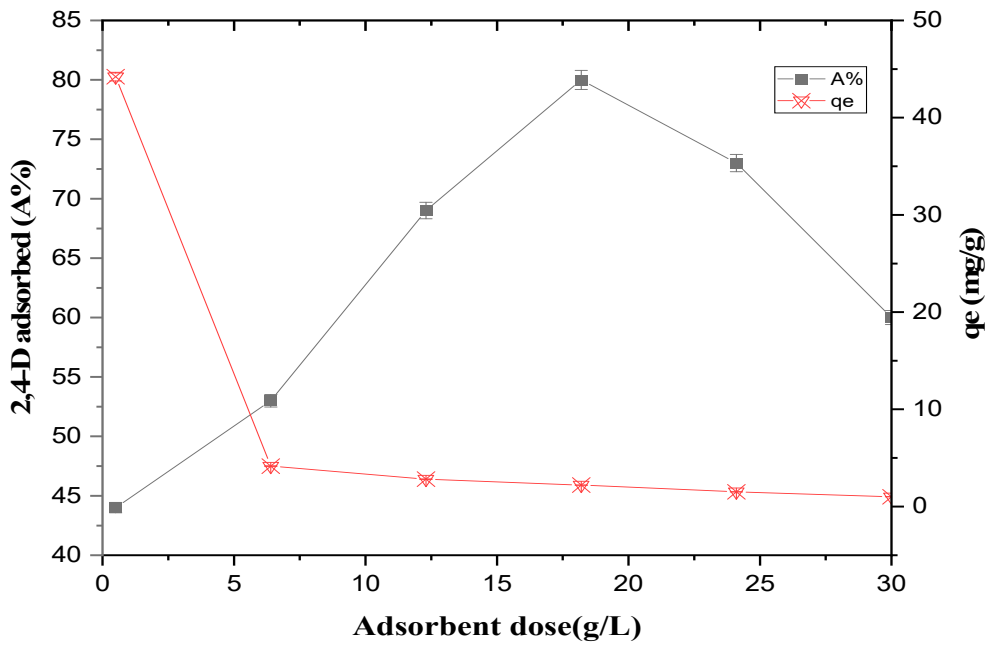

Figure 6. Effect of TMS dose on 2,4-D percentage removal (A%) and adsorption capacity (q_e). The standard deviation for three different sample runs is shown by the error bars.

3.2.3. Effect of 2,4-D Initial Concentration

By changing the concentration from 0.5 mg/L to 100 mg/L while keeping the other parameters constant, the impact of the 2,4-D initial concentration on its removal was evaluated. Figure 7 shows the 2,4-D adsorption capacity and the percentage of 2,4-D removal at various 2,4-D initial concentrations. The percentage of 2,4-D removal decreased from 80 to 22% with the rise in the 2,4-D initial concentration from 0.5 to 100 mg/L. This reduction could be the result of the 2,4-D saturating the available active sites on the TMS [37]. The adsorption capacity rose from 0.03 to 1.78 mg/g with the rise in 2,4-D initial concentration from 0.5 to 80 mg/L; with a further increase to 100 mg/L, it dropped to 1.44 mg/g. The increase in adsorption capacity may be due to the utilization of all the available active sites for adsorption at higher 2,4-D concentrations, a larger mass transfer of driving force, as well as a rise in the number of collisions between the 2,4-D molecules and the TMS [37,38]. In earlier investigations, Ref. [13], the 2,4-D removal results were similar when bagasse fly ash was used as an adsorbent.

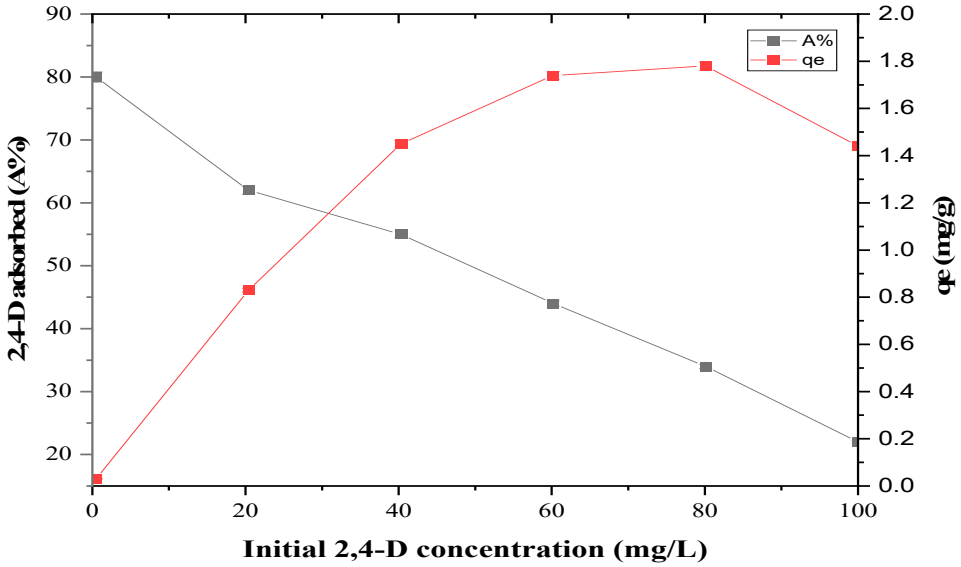

Figure 7. Effect of 2,4-D initial concentration on 2,4-D percentage removal (A%) and adsorption capacity (q_e). For three different sample runs, the error bars show the standard deviation.

3.2.4. Effect of Contact Time

The results of a study on the effect of time on 2,4-D adsorption by TMS are depicted graphically in Figure 8. The results show that the 2,4-D percentage removal rapidly increased from 0 to 80% when the contact time increased from 0 to 180 min. After 180 min of equilibration, its rate becomes constant. The equilibrium contact time showed a very quick reaction as compared to other findings, such as 240 min [39] and 4 days [40], for activated carbon generated from date stones and granular activated carbon, respectively.

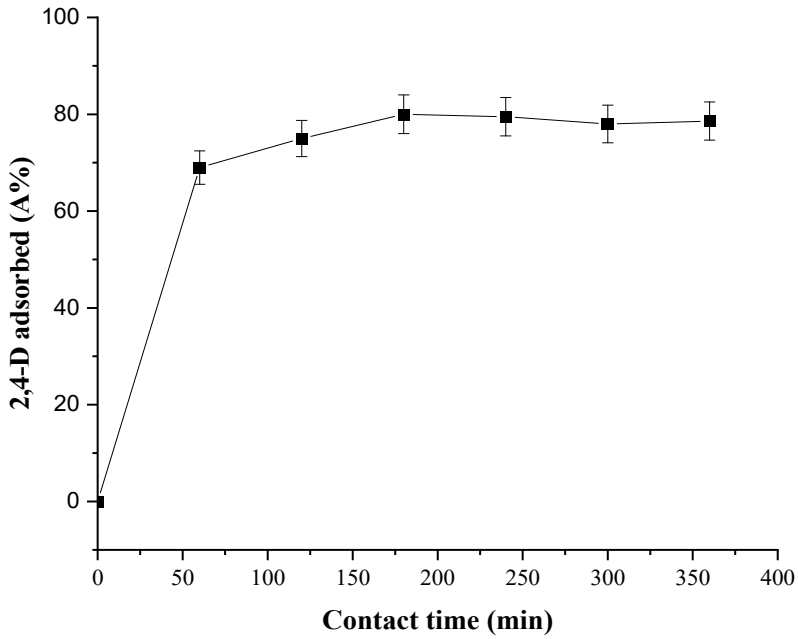

Figure 8. Effect of contact time on 2,4-D percentage removal. The error bars show the standard deviation for three different sample runs.

3.2.5. Adsorption Kinetics

The 2,4-D adsorption on TMS is explained by the pseudo-first-order, pseudo-second-order, and intraparticle diffusion theories (Table 3). As demonstrated in Table 3 and Figure 9, the pseudo-second-order kinetic model fit the adsorption kinetic data with a 0.99 correlation

coefficient, and the computed adsorption capacity ($q_{e,cal}$) and experimental adsorption capacity were similar ($q_{e,exp}$). The rate constant, K_2, dropped from 0.63 to 0.103 with an increased starting concentration, suggesting that 2,4-D adsorption was proceeding more quickly [25]. Table 3 demonstrates that greater concentrations had a higher diffusion rate (K_p) value than lower concentrations, indicating that higher concentrations had a faster diffusion rate than lower concentrations [41].

Table 3. Pseudo-first-order, pseudo-second-order, and intraparticle diffusion characteristics of 2,4-D adsorption on TMS.

Model	Parameters	2,4-D Concentration (mg/L)	
		20	**50.25**
Pseudo-first -order	$q_{e,exp}$ (mg/g)	0.92	2.64
	K_1 (min^{-1})	−1.71	−2.3
	$q_{e,cal}$ (mg/g)	0.92	0.36
	R^2	0.53	0.35
Pseudo-second-order	K_2 g/(mg.min)	0.63	0.103
	$q_{e,cal}$ (mg/g)	0.87	2.62
	R^2	0.99	0.99
Intraparticle diffusion	Kp mg/(g.$min^{0.5}$)	0.043	0.128
	C (mg/g)	0.214	0.631
	R^2	0.73	0.75

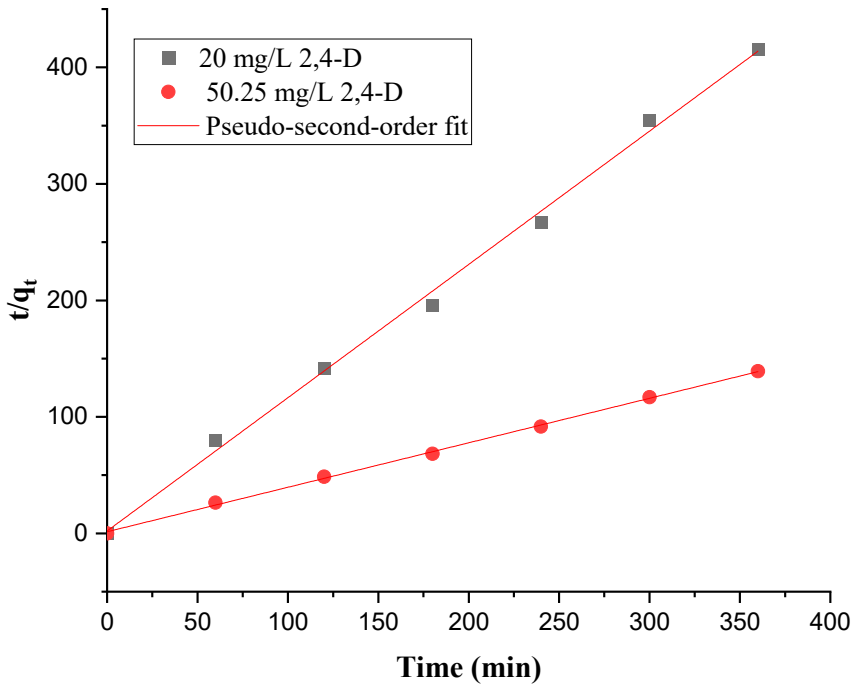

Figure 9. Pseudo-second-order fits for the sorption of 2,4-D on TMS.

3.2.6. Adsorption Isotherm

The Freundlich and Langmuir models were used to examine the equilibrium data. The Langmuir isotherm predicts a monolayer adsorption process over the homogeneous surface sites, whereas the Freundlich isotherm predicts multilayer adsorption of a solution on the heterogeneous surface sites of a solid [42]. The equilibrium 2,4-D adsorption isotherm plots are graphically displayed in Figures 10 and 11, and the equilibrium constant values calculated using the isotherm models are provided in Table 4. The value of the determination coefficients ($R^2 > 0.9687$) was proved using the Langmuir isotherm. The 2,4-D adsorption on the TMS equilibrium data is thus better described by the Langmuir isotherm

model. By analyzing the key elements of the Langmuir isotherm, which are denoted by a dimensionless constant separation factor, R_L, and calculated by $R_L = 1/(1 + bC_0)$, it is possible to determine the type of the adsorption isotherm [43], where b (L/mg) is the Langmuir constant and C_0 (mg/L) is the initial 2,4-D concentration (Table 5). The value of R_L demonstrates that the adsorption process is unfavorable if $R_L > 1$, linear if $R_L = 1$, favorable if $0 < R_L < 1$, and irreversible if $R_L = 0$. Therefore, the obtained value of R_L (0.25), which is within the range of 0–1, shows the favorable equilibrium adsorption of 2,4-D on the TMS [43].

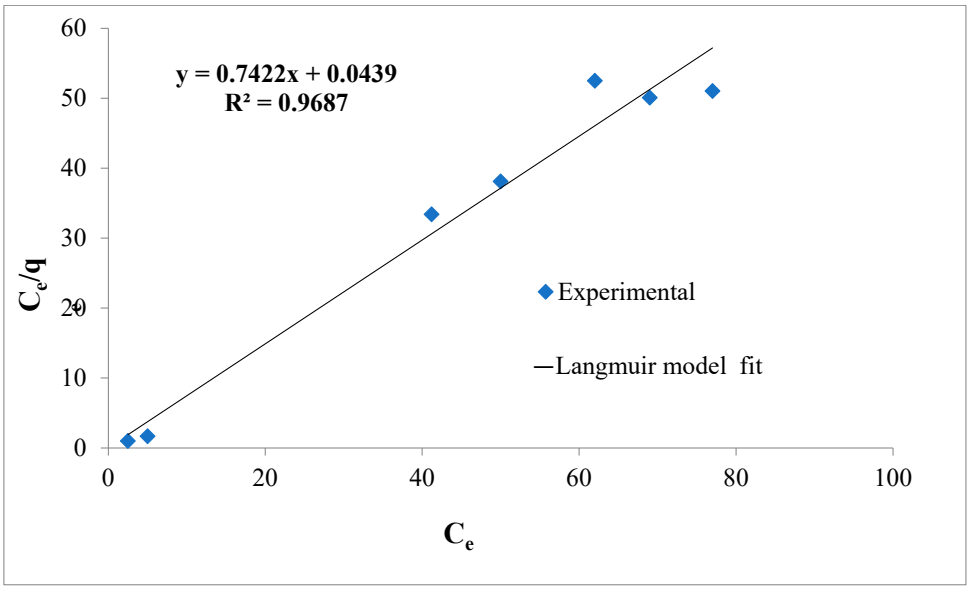

Figure 10. Langmuir adsorption isotherm model for 2,4-D on TMS.

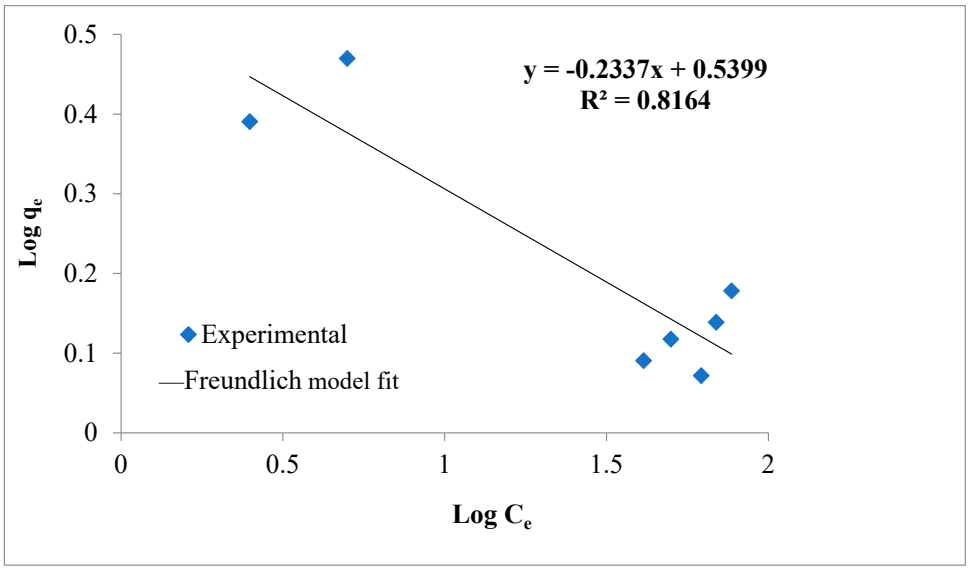

Figure 11. Freundlich adsorption isotherm model for 2,4-D on TMS.

Table 4. Isotherm variables for 2,4-D adsorption on TMS.

Isotherm/Models	Freundlich Constants			Langmuir Constants			
Variables	**1/n**	**K**	**R^2**	**q_{max} (mg/g)**	**K_L (L/mg)**	**R_L**	**R^2**
Values	−0.23	3.47	0.8164	22.78	0.06	0.25	0.9687

Table 5. Comparison of 2,4-D Langmuir adsorption capacities of different adsorbents.

Adsorbent	Adsorption Capacity (mg/g)	References
Rice husk ash	1.4	[35]
Activated carbon from corncob	95.26	[13]
Mustard plant ash	0.76	[44]
Bentonite clay	136.14	[45]
Granular activated carbon	0.688	[46]
Cladium mariscus	65.58	[7]
Bagasse fly ash	5.63	[37]
Termite mound soil	22.78	This study

3.3. Central Composite Design (CCD)

The traditional "one-at-a-time" method of optimization is time-consuming and impractical for achieving the genuine optimum state, due to poor interaction between the factors [47]. This is why the combined influence of the factors on the response was optimized and examined using CCD under RSM. Table 6 displays an experimental measurement for the percentage of 2,4-D removed from agricultural leachate. At a contact time of 180.5 min, pH 2, and an adsorbent dose of 15.25 g, 89.6% of the adsorptive removal was recorded, while at a contact time of 360 min, pH 9, and 0.5 g of adsorbent dosage, 25% of the removal was discovered. Table 7 provides the 2,4-D removal ANOVA. All the individual factors and their combinations demonstrated statistically significant beneficial effects on 2,4-D adsorption, as shown by the influence factors shown in the ANOVA (Table 6). The model's F value was 152.76 and its p-value was less than 0.05, which suggests that the model is significant, according to the findings of the Design–Expert 13 test. If a model's p-value (significance probability value) is less than 0.05, it is deemed significant. The coefficient of determination (R^2 = 0.9972) and the adjusted R^2 (0.9907) are in close agreement with the predicted R^2 (0.8836) value. According to the p-values in Table 7, the linear terms A, B, C, and D, and their interactions AB, AC, AD, BD, and CD, as well as the quadratic terms A^2, B^2, C^2, and D^2, are significant model terms. Figure 12 displays the actual and projected plots. The data points on the plot were reasonably dispersed close to the straight line, as seen in Figure 12, demonstrating a reasonable match between the experimental and the anticipated response values. Additionally, the outcome indicated that the quadratic model was capable of correctly predicting the response variables for experimental data.

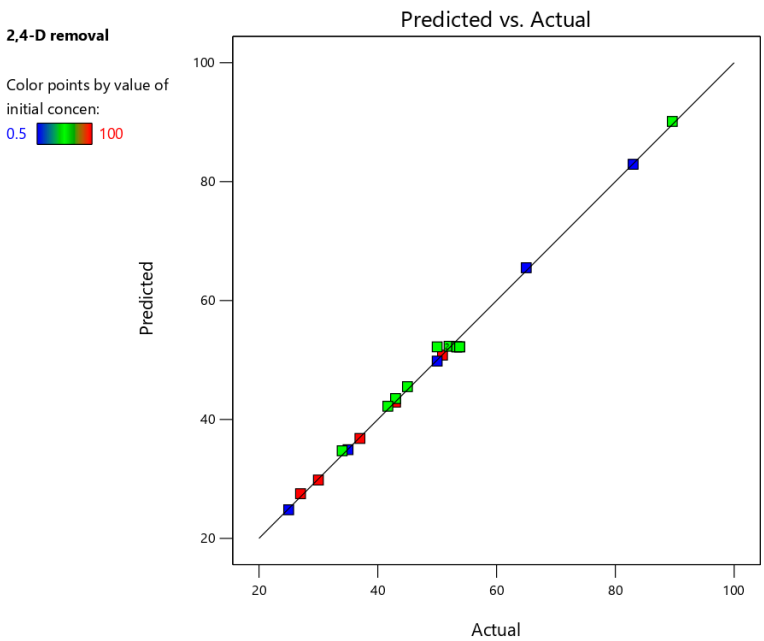

Figure 12. Plot showing 2,4-D absorption using termite mound soil projected values versus actual values.

Table 6. 2,4-D experimental design matrix adsorption percentage values.

Run Order	pH	Contact Time (Min)	Adsorbent Dose (g/L)	Initial 2,4-D Concentration (mg/L)	2,4-D Removal (%)
1	2	360	30	100	50.9
2	2	1	0.5	0.5	50
3	5.5	180.5	15.25	33.4	65
4	9	1	0.5	100	37
5	5.5	180.5	15.25	50.25	53.3
6	5.5	180.5	15.25	50.25	53.8
7	5.5	121.4	15.25	50.25	43
8	2	360	0.5	100	30
9	9	360	30	0.5	35
10	5.5	180.5	40.1	50.25	52
11	12.5	180.5	15.25	50.25	45
12	2	180.5	15.25	50.25	89.6
13	5.5	180.5	15.25	133.9	27
14	5.5	180.5	15.25	50.25	50
15	5.5	180.5	9.6	50.25	50
16	5.5	482.4	15.25	50.25	34
17	1.5	1	30	0.5	83
18	5.5	180.5	15.25	50.25	50.1
19	9	1	30	100	43
20	5.5	180.5	15.25	50.25	50
21	9	360	0.5	0.5	25

Table 7. Analysis of variance (ANOVA), test of significance for 2,4-D adsorption on termite mound soil.

Source	Sum of Squares	Df	Mean Square	F-Value	*p*-Value	
Model	5261.85	14	375.85	152.76	<0.0001	Significant
A-pH	1307.51	1	1307.51	531.41	<0.0001	
B-contact time	69.63	1	69.63	28.30	0.0018	
C-adsorbent dose	628.45	1	628.45	255.42	<0.0001	
D-initial concentration	957.11	1	957.11	389.00	<0.0001	
AB	359.40	1	359.40	146.07	< 0.0001	
AC	179.55	1	179.55	72.98	0.0001	
AD	111.89	1	111.89	45.48	0.0005	
BC	8.20	1	8.20	3.33	0.1177	
BD	273.01	1	273.01	110.96	<0.0001	
CD	32.40	1	32.40	13.17	0.0110	
A^2	622.12	1	622.12	252.85	<0.0001	
B^2	222.66	1	222.66	90.50	<0.0001	
C^2	192.74	1	192.74	78.34	0.0001	
D^2	82.63	1	82.63	33.58	0.0012	
Residual	14.76	6	2.46			
Lack of Fit	4.42	2	2.21	0.8551	0.4907	not significant
Pure Error	10.34	4	2.59			
Cor Total	5276.61		R^2	0.9972		
Std. Dev.	1.57					
Mean	48.35		Adjusted R^2	0.9907		
C.V.%	3.24		Predicted R^2	0.8836		
			Adeq Precision	49.2631		

Interaction between the Relevant Parameters

To calculate the combined impact of the independent factors on the adsorption efficiency, three-dimensional response surface plots were created. Figure 13 depicts the plots. Figure 13A illustrates how the contact duration and pH affect the elimination of 2,4-D. At pH 2, with a 180-minute contact duration, the maximum 2,4-D elimination (89.6%) was noted. In the interaction between the adsorbent dose and the pH (Figure 13B), at pH 2, the

range of adsorbent dosages within which the maximum 2,4-D removal was achieved was 12.3 g/L to 18.2 g/L. The interaction between the pH and the initial concentration is seen in Figure 13C, with the maximum 2,4-D removal occurring at pH 2 and initial values between 20 mg/L and 51 mg/L.

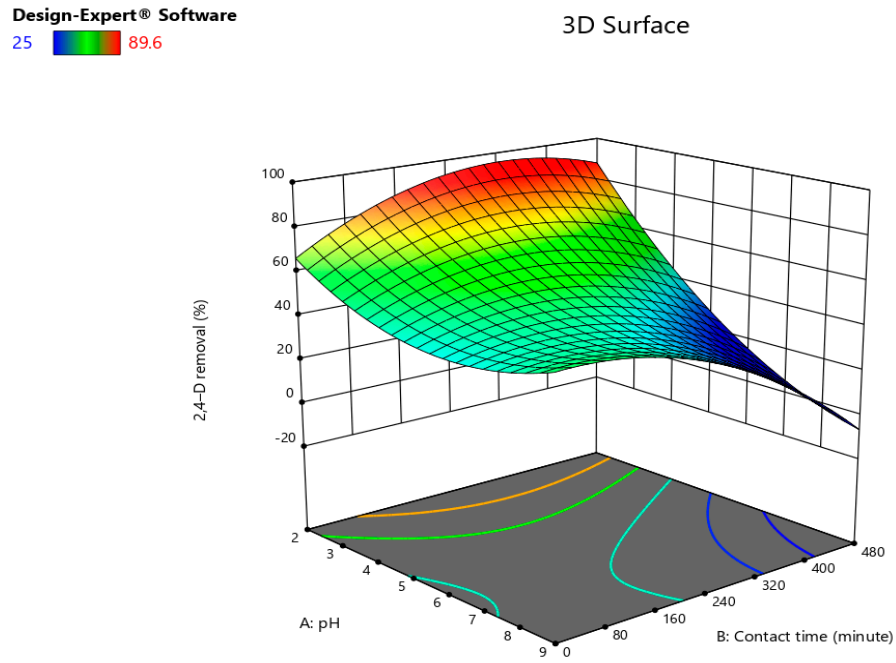

(**A**)

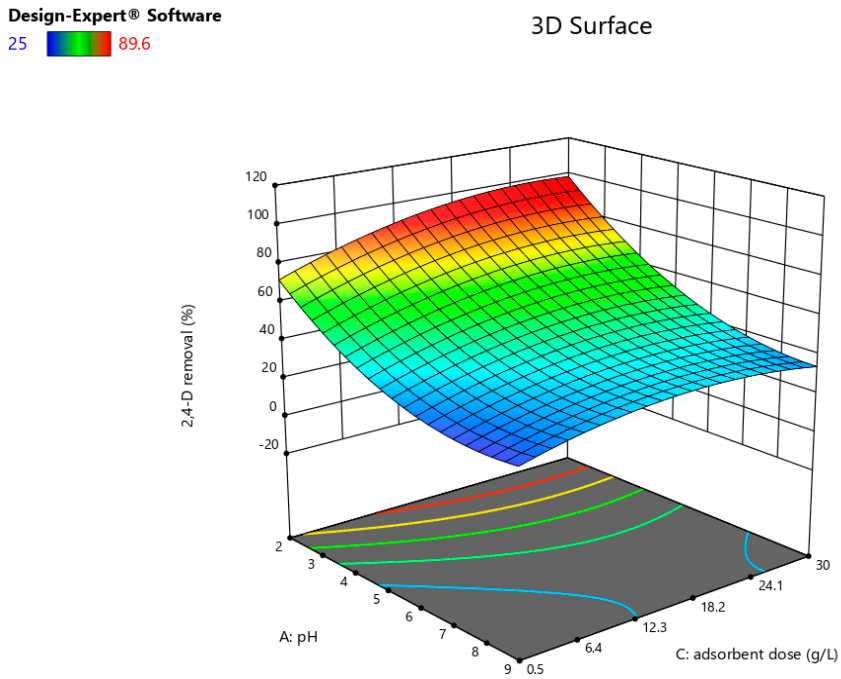

(**B**)

Figure 13. *Cont.*

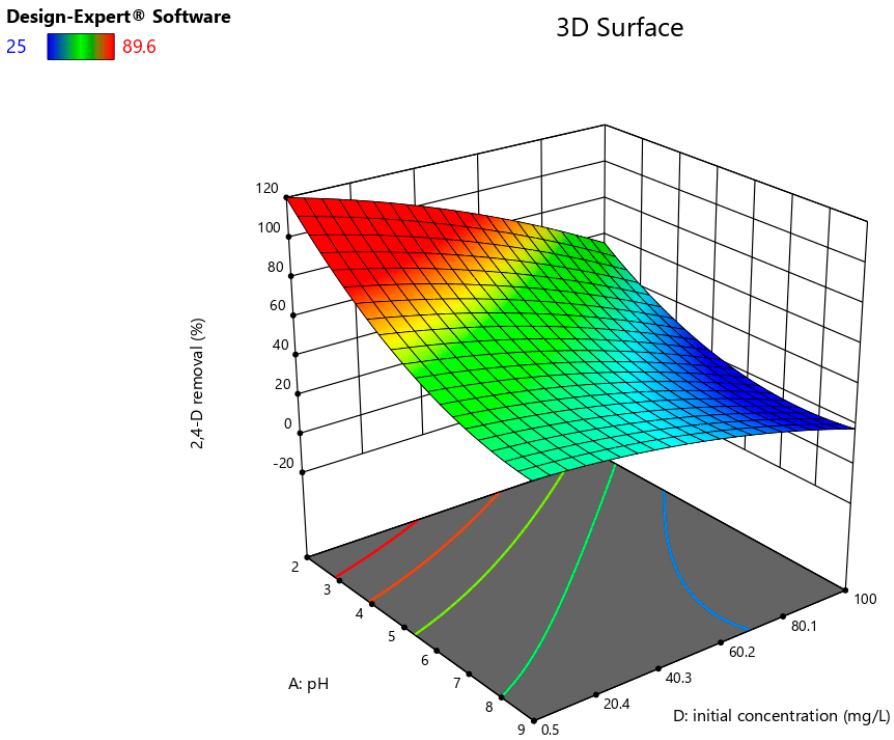

(**C**)

Figure 13. The interaction between (**A**) contact time and pH. (**B**) adsorbent dose and pH, and (**C**) initial concentration and pH, illustrating their effect on 2,4-D adsorption.

4. Conclusions

The aim of the investigation was to establish TMS's capacity for sorbing 2,4-D from agricultural leachate. Additionally, the adjustment of the operational variables to increase the 2,4-D adsorption on the TMS was investigated. The impact of four independent factors on the 2,4-D sorption by TMS from agricultural leachate was investigated using the RSM model, based on a half-factorial CCD. The most important variables for 2,4-D removal, according to the quadratic model employed for the response surface analysis, were pH, contact time, adsorbent dose, and initial 2,4-D concentration. The results showed that a pH of 2, contact time of 180.5 min, adsorbent dose of 15.25 g/L, and an initial 2,4-D concentration of 50.25 mg/L were the ideal adsorption conditions, and the sorption process followed pseudo-second-order kinetics. Moreover, the data from the Langmuir isotherm model (R^2 = 0.9687) revealed that the Langmuir isotherm's qmax was 22.78 mg/g. Overall, it can be said that TMS, which is widely available on agricultural land in Ethiopia but is typically regarded as waste, has the ability to remove 2,4-D from agricultural leachate. However, before reaching a firm conclusion for practical application, further investigation is required on the desorption and reuse of spent TMS, as well as the TMS 2,4-D removal potential from real wastewater.

Author Contributions: Investigation, Y.D.; supervision, E.A. and Z.W.; writing—original draft, Y.D.; writing—review and editing, Y.D., E.A., Z.W., W.B. and B.L. All authors have read and agreed to the published version of the manuscript.

Funding: This research received no external funding.

Data Availability Statement: The data used in this study are available from first author at reasonable trequest.

Acknowledgments: The Ethiopian Institute of Agricultural Research (EIAR) and the Addis Ababa Science and Technology University provided funding for this research. The lab facilities provided by the Addis Ababa Science and Technology University and the EIAR Food Science and Nutrition Research Directorate are gratefully acknowledged.

Conflicts of Interest: The authors declare no conflict of interest.

References

1. Rani, K.; Dhania, G. Bioremediation and biodegradation of pesticide from contaminated soil and water—A noval approach. *Int. J. Curr. Microbiol. App. Sci.* **2014**, *3*, 23–33.
2. Islam, F.; Wang, J.; Farooq, M.A.; Khan, M.S.; Xu, L.; Zhu, J.; Zhao, M.; Muños, S.; Li, Q.X.; Zhou, W. Potential impact of the herbicide 2,4-dichlorophenoxyacetic acid on human and ecosystems. *Environ. Int.* **2018**, *111*, 332–351. [CrossRef] [PubMed]
3. Goscianska, J.; Olejnik, A. Removal of 2,4-D herbicide from aqueous solution by aminosilane-grafted mesoporous carbons. *Adsorption* **2019**, *25*, 345–355. [CrossRef]
4. Souza, F.; Saéz, C.; Llanos, J.; Lanza, M.R.; Cañizares, P.; Rodrigo, M.A. Solar-powered electrokinetic remediation for the treatment of soil polluted with the herbicide 2,4-D. *Electrochim. Acta* **2016**, *190*, 371–377. [CrossRef]
5. Mustafa, Y.A.; Abdul-Hameed, H.M.; Razak, Z.A. Biodegradation of 2,4-dichlorophenoxyacetic acid contaminated soil in a roller slurry bioreactor. *CLEAN-Soil Air Water* **2015**, *43*, 1241–1247. [CrossRef]
6. Bazrafshan, E.; KORD, M.F.; Faridi, H.; Farzadkia, M.; Sargazi, S.; Sohrabi, A. Removal of 2,4-dichlorophenoxyacetic acid (2,4-D) from aqueous environments using single-walled carbon nanotubes. *Health Scope* **2013**, *2*, 39–46. [CrossRef]
7. Bartczak, P.; Żółtowska, S.; Norman, M.; Klapiszewski, Ł.; Zdarta, J.; Komosa, A.; Kitowski, I.; Ciesielczyk, F.; Jesionowski, T. Saw-sedge Cladium mariscus as a functional low-cost adsorbent for effective removal of 2,4-dichlorophenoxyacetic acid from aqueous systems. *Adsorption* **2016**, *22*, 517–529. [CrossRef]
8. Trivedi, N.S.; Kharkar, R.A.; Mandavgane, S.A. 2,4-Dichlorophenoxyacetic acid adsorption on adsorbent prepared from groundnut shell: Effect of preparation conditions on equilibrium adsorption capacity. *Arab. J. Chem.* **2019**, *12*, 4541–4549. [CrossRef]
9. Trivedi, N.S.; Mandavgane, S.A. Fundamentals of 2,4 dichlorophenoxyacetic acid removal from aqueous solutions. *Sep. Purif. Rev.* **2018**, *47*, 337–354. [CrossRef]
10. Chen, H.; Zhang, Z.; Yang, Z.; Yang, Q.; Li, B.; Bai, Z. Heterogeneous fenton-like catalytic degradation of 2,4-dichlorophenoxyacetic acid in water with FeS. *Chem. Eng. J.* **2015**, *273*, 481–489. [CrossRef]
11. Guleri, S.; Singh, K.; Kaushik, R.; Dhankar, R.; Tiwari, A. Phycoremediation: A novel and synergistic approach in wastewater remediation. *J. Microbiol. Biotechnol. Food Sci.* **2020**, *10*, 98–106. [CrossRef]
12. Zhou, T.; Fang, L.; Wang, X.; Han, M.; Zhang, S.; Han, R. Adsorption of the herbicide 2,4-dichlorophenoxyacetic acid by Fe-crosslinked chitosan complex in batch mode. *Desalin Water Treat.* **2017**, *70*, 294–301. [CrossRef]
13. Deokar, S.K.; Mandavgane, S.A.; Kulkarni, B.D. Adsorptive removal of 2,4-dichlorophenoxyacetic acid from aqueous solution using bagasse fly ash as adsorbent in batch and packed-bed techniques. *Clean Technol. Environ. Policy* **2016**, *18*, 1971–1983. [CrossRef]
14. Reddy, D.H.K.; Lee, S.-M. Application of magnetic chitosan composites for the removal of toxic metal and dyes from aqueous solutions. *Adv. Colloid Interface Sci.* **2013**, *201*, 68–93. [CrossRef]
15. Tilahun, A.; Kebede, F.; Yamoah, C.; Erens, H.; Mujinya, B.; Verdoodt, A.; Van Ranst, E. Quantifying the masses of Macrotermes subhyalinus mounds and evaluating their use as a soil amendment. *Agric. Ecosyst. Environ.* **2012**, *157*, 54–59. [CrossRef]
16. Chauhan, A.K.; Maheshwari, D.K.; Dheeman, S.; Bajpai, V.K. Termitarium-inhabiting Bacillus spp. enhanced plant growth and bioactive component in turmeric (*Curcuma longa* L.). *Curr. Microbiol.* **2017**, *74*, 184–192. [CrossRef]
17. Enagbonma, B.J.; Babalola, O.O. Environmental sustainability: A review of termite mound soil material and its bacteria. *Sustainability* **2019**, *11*, 3847. [CrossRef]
18. Amiri, M.J.; Bahrami, M.; Beigzadeh, B.; Gil, A. A response surface methodology for optimization of 2,4-dichlorophenoxyacetic acid removal from synthetic and drainage water: A comparative study. *Environ. Sci. Pollut. Res.* **2018**, *25*, 34277–34293. [CrossRef]
19. Moradi, M.; Fazlzadehdavil, M.; Pirsaheb, M.; Mansouri, Y.; Khosravi, T.; Sharafi, K. Response surface methodology (RSM) and its application for optimization of ammonium ions removal from aqueous solutions by pumice as a natural and low cost adsorbent. *Arch. Environ. Prot.* **2016**, *42*, 33–43. [CrossRef]
20. Appel, C.; Ma, L. Concentration, pH, and surface charge effects on cadmium and lead sorption in three tropical soils. *J. Environ. Qual.* **2002**, *31*, 581–589. [CrossRef]
21. Mahmood, T.; Saddique, M.T.; Naeem, A.; Westerhoff, P.; Mustafa, S.; Alum, A. Comparison of different methods for the point of zero charge determination of NiO. *Ind. Eng. Chem. Res.* **2011**, *50*, 10017–10023. [CrossRef]
22. Tebeje, A.; Worku, Z.; Nkambule, T.; Fito, J. Adsorption of chemical oxygen demand from textile industrial wastewater through locally prepared bentonite adsorbent. *Int. J. Environ. Sci. Technol.* **2022**, *19*, 1893–1906. [CrossRef]
23. Bedada, D.; Angassa, K.; Tiruneh, A.; Kloos, H.; Fito, J. Chromium removal from tannery wastewater through activated carbon produced from Parthenium hysterophorus weed. *Energy Ecol. Environ.* **2020**, *5*, 184–195. [CrossRef]
24. OECD. *106: Adsorption–Desorption Using a Batch Equilibrium Method*; OECD: Paris, France, 2000. [CrossRef]

25. Fufa, F.; Alemayehu, E.; Lennartz, B. Sorptive removal of arsenate using termite mound. *J. Environ. Manag.* **2014**, *132*, 188–196. [CrossRef]
26. Mohamed, H.S.; Soliman, N.; Abdelrheem, D.A.; Ramadan, A.A.; Elghandour, A.H.; Ahmed, S.A. Adsorption of Cd^{2+} and Cr^{3+} ions from aqueous solutions by using residue of Padina gymnospora waste as promising low-cost adsorbent. *Heliyon* **2019**, *5*, e01287. [CrossRef]
27. Vyas, B.; Kumar Singh, A.; Singh Cameotra, S. Sorption behaviour of maneb in the agriculture soils and its correlation with soil properties. *Int. J. Eng. Sci.* **2015**, *1*, 1–8.
28. Taktak, F.; İlbay, Z.; Şahin, S. Evaluation of 2,4-D removal via activated carbon from pomegranate husk/polymer composite hydrogel: Optimization of process parameters through face centered composite design. *Korean J. Chem. Eng.* **2015**, *32*, 1879–1888. [CrossRef]
29. Huang, L.; Kong, J.; Wang, W.; Zhang, C.; Niu, S.; Gao, B. Study on Fe (III) and Mn (II) modified activated carbons derived from Zizania latifolia to removal basic fuchsin. *Desalination* **2012**, *286*, 268–276. [CrossRef]
30. Du Changwen, M.F.; Yuzhen, L.; Jianmin, Z. 6 Soil Fertility Assessed by Infrared Spectroscopy. *Soil-Specif. Farming: Precis. Agric.* **2015**, *22*, 155.
31. Hospodarova, V.; Singovszka, E.; Stevulova, N. Characterization of cellulosic fibers by FTIR spectroscopy for their further implementation to building materials. *Am. J. Anal. Chem.* **2018**, *9*, 303–310. [CrossRef]
32. Kajjumba, G.W.; Yıldırım, E.; Aydın, S.; Emik, S.; Ağun, T.; Osra, F.; Wasswa, J. A facile polymerisation of magnetic coal to enhanced phosphate removal from solution. *J. Environ. Manag.* **2019**, *247*, 356–362. [CrossRef]
33. Gülen, J.; Arslan, S. Adsorption of 2,4-D on carbonized chest nut shell. *Phys. Rev. Res. Int.* **2013**, *3*, 531–540.
34. Gupta, V.K.; Ali, I.; Saini, V.K. Adsorption of 2,4-D and carbofuran pesticides using fertilizer and steel industry wastes. *J. Colloid Interface Sci.* **2006**, *299*, 556–563. [CrossRef]
35. Njoku, V.; Hameed, B. Preparation and characterization of activated carbon from corncob by chemical activation with H_3PO_4 for 2,4-dichlorophenoxyacetic acid adsorption. *Chem. Eng. J.* **2011**, *173*, 391–399. [CrossRef]
36. Salman, J.; Njoku, V.; Hameed, B. Batch and fixed-bed adsorption of 2,4-dichlorophenoxyacetic acid onto oil palm frond activated carbon. *Chem. Eng. J.* **2011**, *174*, 33–40. [CrossRef]
37. Hameed, B.; Salman, J.; Ahmad, A. Adsorption isotherm and kinetic modeling of 2,4-D pesticide on activated carbon derived from date stones. *J. Hazard. Mater.* **2009**, *163*, 121–126. [CrossRef]
38. Aksu, Z.; Gönen, F. Biosorption of phenol by immobilized activated sludge in a continuous packed bed: Prediction of breakthrough curves. *Process Biochem.* **2004**, *39*, 599–613. [CrossRef]
39. Zhao, S.; Feng, C.; Huang, X.; Li, B.; Niu, J.; Shen, Z. Role of uniform pore structure and high positive charges in the arsenate adsorption performance of Al13-modified montmorillonite. *J. Hazard. Mater.* **2012**, *203*, 317–325. [CrossRef]
40. Wang, S.; Boyjoo, Y.; Choueib, A. A comparative study of dye removal using fly ash treated by different methods. *Chemosphere* **2005**, *60*, 1401–1407. [CrossRef]
41. Solaimany Nazar, A.R.; Jokar Baloochi, S.; Farhadian, M.; Goshadrou, A. 2,4-dichlorophenoxyacetic acid adsorption from contaminated water through activated carbon reclaimed with zero-valent iron and titanium dioxide. *Sci. Iran.* **2018**, *25*, 1395–1411.
42. Deokar, S.K.; Mandavgane, S.A. Rice husk ash for fast removal of 2,4-dichlorophenoxyacetic acid from aqueous solution. *Adsorpt. Sci. Technol.* **2015**, *33*, 429–440. [CrossRef]
43. Trivedi, N.S.; Mandavgane, S.A.; Kulkarni, B.D. Mustard plant ash: A source of micronutrient and an adsorbent for removal of 2,4-dichlorophenoxyacetic acid. *Environ. Sci. Pollut. Res.* **2016**, *23*, 20087–20099. [CrossRef] [PubMed]
44. de Souza, F.M.; Dos Santos, O.A.A.; Vieira, M.G.A. Adsorption of herbicide 2,4-D from aqueous solution using organo-modified bentonite clay. *Environ. Sci. Pollut. Res.* **2019**, *26*, 18329–18342. [CrossRef] [PubMed]
45. Dehghani, M.; Nasseri, S.; Karamimanesh, M. Removal of 2,4-Dichlorophenolyxacetic acid (2,4-D) herbicide in the aqueous phase using modified granular activated carbon. *J. Environ. Health Sci. Eng.* **2014**, *12*, 28. [CrossRef]
46. Zolgharnein, J.; Shahmoradi, A.; Ghasemi, J. Pesticides removal using conventional and low-cost adsorbents: A review. *CLEAN-Soil Air Water* **2011**, *39*, 1105–1119. [CrossRef]
47. Ani, J.; Okoro, U.; Aneke, L.; Onukwuli, O.; Obi, I.; Akpomie, K.; Ofomatah, A. Application of response surface methodology for optimization of dissolved solids adsorption by activated coal. *Appl. Water Sci.* **2019**, *9*, 60. [CrossRef]